Role of the geomorphic setting in controlling groundwater-surface water exchanges in riverine wetlands – A case study from two southern Québec rivers (Canada)

Marie Larocque[1]*, Pascale M. Biron[2], Thomas Buffin-Bélanger[3], Michael Needelman[1], Claude-André Cloutier[3] and Jeffrey M. McKenzie[4]

[1] Centre de recherche GÉOTOP, département des sciences de la Terre et de l'atmosphère, Université du Québec à Montréal, Montréal, Québec H2C 3P8

[2] Department of Geography, Planning and Environment, Concordia University, Montréal, Québec, Canada

[3] Département de biologie, chimie et géographie, Université du Québec à Rimouski, Rimouski, Québec, Canada

[4] Department of Earth and Planetary Sciences, McGill University, Montréal

* Corresponding author

For the use of the editors

Paper #:

Submitted on:

Accepted on:

Application - Research – Commentary – Book Review:

Copyright Held by:

T2012

Abstract

There is great interest worldwide to reconnect floodplain wetlands to their rivers. Whilst the surface water connection between rivers and wetlands is fairly well understood, the linkages via groundwater are not well known. In this study, it is hypothesized that the significance of the groundwater pathways between rivers and wetlands is largely determined by the geomorphic setting of the riverine corridor. This was tested by measuring the response of water levels and temperatures in floodplain groundwater and in wetlands to river pulses in two geomorphologically-distinct riverine corridors in

Southern Québec. In the De la Roche River (DLR; 145 km^2), the floodplain is narrow and the alluvial sediments consist of sandy silt (wetland A; abandoned meander) or clayey silt (wetland B; stable floodplain), depending on the location. During within-channel floods, exchanges of water between the river and the floodplain are limited to some bank recharge where the alluvial sediments are permeable, and over-bank storage where the sediments are finer. Water levels in the DLR floodplain wetlands were controlled by a combination of over-bank flow and groundwater discharge from adjacent uplands. In the Matane River (1678 km^2), the floodplain substrate is coarser, and the floodplain is wider and has a meandering planform geometry. The response of the Matane River wetland during floods shows storage of water due to a groundwater flood wave. This response of the wetland to within-channel flood pulses could play a role in downstream flood attenuation. In this river, the presence of river infiltration in this floodplain was also illustrated by the warming of floodplain groundwater during flood pulses. This study has shown with three distinct examples how riverine wetlands can be connected to their rivers via either a surface or subsurface pathway depending on the geomorphic setting of the riverine corridor.

Keywords: geomorphic setting, wetland, aquifer, river, Québec (Canada)

Résumé

Il existe un intérêt croissant pour reconnecter les milieux humides riverains aux rivières. Même si les échanges entre les rivières et les milieux humides sont relativement bien compris, les liens avec les eaux souterraines demeurent méconnus. Cette étude visait à montrer que l'importance des connexions souterraines entre rivières et milieu humides est déterminée par le contexte géomorphologique du corridor riverain. La réponse de la nappe des milieux humides dans la plaine inondable aux variations de niveaux dans la rivière a été étudiée dans deux corridors riverains de contextes géomorphologiques distincts du Québec méridional. Dans la rivière De la Roche (DLR; 145 km^2), la plaine inondable est étroite et composée de silts sableux (milieu humide A; méandre abandonné) ou de silts argileux (milieu humide B; plaine inondable stable). La plaine inondable emmagasine un certain volume d'eau aux endroits où les sédiments sont perméables et stocke l'eau en surface où les sédiments sont plus fins. Les niveaux dans les milieux

humides de la rivière DLR sont contrôlés par une combinaison de stockage de surface et par des apports d'eau de l'aquifère adjacent. Sur la rivière Matane (1678 km^2), les sédiments sont plus grossiers, la plaine inondable est plus large et montre une géométrie complexe d'anciens méandres. La réponse du milieu humide de la rivière Matane aux crues traduit un emmagasinement engendré par une vague souterraine qui pourrait jouer un rôle important dans l'atténuation des crues en aval. L'infiltration de l'eau de rivière dans la plaine inondable de la rivière Matane a été mise en évidence par le réchauffement de l'eau souterraine à proximité de la rivière lors des crues. Cette étude a montré comment les milieux humides riverains peuvent être connectés aux cours d'eau par l'emmagasinement en surface ou par des connexions souterraines, en fonction du contexte géomorphologique du corridor riverain.

Introduction

Integrated watershed management is increasingly recognizing that rivers are not linear features confined in a channel, but that their spatial and temporal dynamics define a larger and variable space that needs to be determined for adequate river management. The river corridor (Kline and Cahoon 2010), the fluvial territory (Ollero 2010), and the freedom space for rivers (Biron et al. 2014; Buffin-Bélanger et al. 2015) are examples of river space concepts guided by the analysis of geomorphological and hydrological processes occurring on the floodplain. However, these river space concepts pay less attention to hydrogeological processes occurring *within* the floodplain. To develop a comprehensive river corridor management approach, there is a need to better consider the connections between the river and the alluvial aquifer, notably through wetlands which can contribute to flood mitigation (Bullock and Acreman 2003; Piégay et al. 2005; Arnaud-Fassetta et al. 2009), lessen the severity of low flows, filter underground contaminants (Emmett et al. 1994; Verhoeven et al. 2006) and provide healthy ecosystems.

Hydrological connections between aquifers, wetlands and rivers can be defined using response time and bank storage, both of which are influenced by the hydraulic conductivity of the deposits and by the morphological features of the floodplain. As residence time is directly influenced by connectivity, it may affect the wetland potential for nitrogen removal via denitrification (Racchetti et al. 2011; Roley et al. 2012). Aquatic and wetland biodiversity are also often related to hydrological connections (Phillips 2013) with groundwater-connected wetlands offering relatively constant humidity and temperature conditions, due to more stable water levels (Lowry et al. 2007). Connectivity is also strongly related to abandoned channel water bodies such as meander loops (Phillips 2013), and there is often strong hydrological connection between these two entities. As such, it is a dynamic system which can evolve over time following geomorphic evolution of the river channel (Amoros and Bornette 2002; Phillips 2013). New oxbow lakes tend to vary in stage in a similar way to the river channel. However, older oxbow lakes, even if located very close to the channel, can be essentially isolated from it, at least in terms of surface water (Hudson 2010). Channel-floodplain connections are thus complex and cannot simply be determined by variables such as distance from channel and differences in elevation between the channel and the wetland (Phillips 2013). More research is needed to define a general typology that would include the geomorphic setting.

Although river-aquifer connections through baseflows have been increasingly studied in the last decade, there is a lack of literature on how these connections occur in the presence of wetlands, particularly when wetlands are formed through meander cut-off (Džubáková et al. 2015). A key question concerns the drivers of the surface water level regime of floodplain wetlands, as it is not clear if these are dominated by rainfall, surface runoff (i.e. over-bank flow), a local river-derived groundwater system, a regional groundwater system or some combination thereof. How important these different sources of water will be for a particular wetland will depend on climate, aquifer properties and geomorphic setting. Most studies so far have either focused on a single wetland, or have assumed a similar hydrologic connectivity for all riverine wetlands. Significant efforts have been made towards developing such a typology for wetlands in general (e.g.: Acreman 2004; Ramsar 2005). However, the significance of the groundwater pathway between rivers and wetlands being largely determined by the geomorphic setting of the riverine corridor, it is necessary to include geomorphology in refining the typology of river-wetland-aquifer connections.

The objective of this research was to provide a better understanding of the role of geomorphology in controlling groundwater-surface water exchanges in riverine wetlands. The study areas were set in two southern Québec rivers with contrasting geomorphological context, the De la Roche River and the Matane River. These contrasted rivers were the focus of a recent hydrogeomorphological study on the implementation of the freedom space approach in river corridors (Biron et al. 2014; Buffin-Bélanger et al. 2015). The De la Roche River is a small river (catchment area 145 km^2) flowing locally on deep-water marine sediments with local abandoned meanders, in an agricultural setting. The Matane River (catchment area 1678 km^2) has a large gravelly floodplain and an irregular meandering planform geometry. To address the research objective, a variety of data were used including river levels, groundwater levels, and water temperature. For the Matane River, this work builds on recent advances on the understanding of the floodwave propagation in the floodplain acquired by Cloutier et al. (2014) and Buffin-Bélanger et al. (2015).

Study sites

Geomorphic settings

The De la Roche (hereafter DLR) River is a fourth-order river located in the Montérégie region, 80 km southeast of Montréal (Canada), close to the state of Vermont, USA (Figure 1). Most of the drainage area is located in Vermont, with only 55 km^2 (out of 145 km^2) in Québec. The highest elevations in the watershed, at 260 m.a.s.l., are located in the upper reaches of the watershed in Vermont. The Québec portion of the longitudinal river profile lies between elevations of approximately 62 to 32 m.a.s.l. at its outlet. The DLR River is located in the St. Lawrence Lowlands, except for the upstream part of the reach which is in the Appalachian plateau. The watershed geology is composed of shale and slate-fractured shale, and to a lesser extent dolomite, sandstone and limestone (Dennis 1964; Stewart 1974; Mehrtens and Dorsey 1987). The surface deposits of the area consist primarily of deep-water marine sediments, till blanket, thin till, reworked till and many sections of exposed rock. There are few areas of alluvium from ancient river terraces due to meandering of the river over the past century. Till covers much of the watershed due to the regional glacial history. The fine, silty and clayey glaciolacustrine deposits resulted from the presence of glacial and proglacial lakes during the deglaciation that began about 13,000 years BP (Dubois et al. 2011). There are also marine sediments reflecting the intrusion of the Champlain Sea about 12,800 to 10,200 years BP (Stewart and McClintock 1969; Cronin 1977). The downstream portion of the DLR River flows mainly on marine sediments. The study reach is much more sinuous than in the upstream portion where it flows directly on till or on the bedrock. The DLR River has an average bankfull width of approximately 12 m and a mean bankfull depth of 1.2 m.

The Matane River is sixth-order river located at the edge of the Gaspésie region, 630 km northeast of Montreal (Figure 1). It is considerably larger than the DLR River (catchment area of 1678 km^2) and much more dynamic. The highest elevations at 1068 m.a.s.l. are located in the eastern part of the watershed. The lowest elevations at the outlet are in the St. Lawrence estuary in the city of Matane. The Matane River watershed is located in the

Appalachian region and is considered semi-alluvial with several bedrock outcrops through its course. The lithology of the Matane valley is deformed sedimentary rock associated with the Appalachian orogenesis from the Cambro-Ordovician period. The Matane River has irregular meandering planform geometry and it flows into a wide semi-alluvial valley cut into quaternary deposits and recent fluvial deposits (Lebuis 1973, Marchand et al. 2014). The floodplain of the Matane River is constructed by the evolution of meander loops, laterally shifting over time. The mean channel width and valley width are 55 m and 475 m, respectively and the bankfull depth in the vicinity of the wetland is 2.8 m. According to borehole data from the valley floor, the average unconsolidated sediment thickness is 49 m. The entire alluvial aquifer of the Matane valley is an unconfined coarse sand/gravel and pebble aquifer with a mean saturated thickness of 46 m, except in the downstream part of the valley, where the alluvial aquifer is overlaid by a 30 m thick silty/clay marine deposit. The presence of a confined aquifer only in the downstream part of the valley suggests that the valley was lately hosted by a glacial tongue connected with a regional ice cap during the latest deglaciation (Marchand et al. 2014). The alluvial aquifer is overtopped by an over-bank sand/silt deposit layer of variable thickness ranging from 0.30 m for the highest topographic forms to 0.75 m within abandoned channels.

Figure 1. a) Québec Province map with location of the two study sites, b) close-up map of the Matane River site (star), and c) close-up view of the two wetlands (WA and WB) of the De la Roche River. The black square in b) and c) indicates the closest gauging station and the darker-grey area represents the watershed area.

Hydrology and hydrogeology

The land use within the DLR watershed is mainly agricultural (mix of crops and feedlots), particularly in the downstream reach, with forested areas upstream. It is one of the main tributaries of the Missisquoi Bay in Lake Champlain. A gauging station is located at the upstream limit of the study reach, downstream of the border with Vermont (CEHQ station 030425; see Figure 1b for location). The mean annual river discharge is 1.1 m^3/s (2001-2012). The maximum observed flow rate is 34.3 m^3/s, while minimum flow rates (baseflows) are on the order of 0.1 m^3/s. The climate normals for the period

1971-2000 indicate an average daily temperature of 6.8 °C and total annual precipitation of 1096 mm (Environment Canada 2013).

The main aquifer associated with the DLR River is unconfined for a large portion of the study area with the exception of the downstream portion of the river where the clayey silts of the Champlain Sea occupy the riverbed. Water table level elevations (height of the water table) vary from approximately 30 m in the downstream meandering portion of the river to over 70 m on the small hilltops that surround the study area (Needelman, 2014; all elevations given as m.a.s.l.). The DLR River drains the aquifer over the entire length of its course in the study area. Results from slug tests indicate that hydraulic conductivities (K) in WB varies from being too low to be measurable to 5.7×10^{-7} m/s, whereas K is somewhat larger in WA with values between 5.3×10^{-7} and 4×10^{-6} m/s (See Fig. 1b for locations; Table 1; Needelman 2014). These values correspond to sandy silt (WA) and to clayey silt (WB) (Freeze and Cherry 1979).

The Matane watershed is mainly forested and the river is known for its iconic Atlantic salmon (*Salmo salar*) population. There is a gauging station located near the mouth of the river (CEHQ station 021601, Figure 1c). The mean annual river discharge is 39 m^3/s (1929–2009), and the bankfull discharge is estimated at 350 m^3/s. Minimum flow rates (considered as baseflows) are on the order of 5 m^3/s. The climate normals for the period 1971-2000 indicate an average daily temperature of 2 °C and total annual precipitation of 1032 mm (Environment Canada, 2013).

A borehole next to the Matane site revealed that the unconfined alluvial aquifer thickness is 47 m. The annual mean water table level at the study site is 58.8 m, whereas the mean floodplain surface elevation is 60.4 m, leaving an unsaturated zone of about 1.6 m (Cloutier et al. 2014). Beyond the floodplain, groundwater levels rapidly increase to 65 m and up to 125 m, 1 km upgradient from the river (MDDELCC, 2014). In the alluvial aquifer within the study site, the general groundwater flow gradient follows the river gradient at low flows. At high flows, however, hydraulic gradients can temporarily be from the river towards the valley wall (Cloutier et al. 2014). At the regional scale, equipotential lines follow that of the topographic settings so that the Matane River is draining the regional aquifer. Results from slug tests indicate that hydraulic conductivities are relatively homogeneous with values ranging from 8.5 x 10^{-4} to 2.1 x 10^{-5} $m.s^{-1}$ (Table 1; Cloutier et al. 2014), which are representative of coarse sand to gravel deposits (Freeze and Cherry 1979).

Table 1. Site hydrogeomorphological conditions

Wetlands

On the DLR River, two riverine wetlands - WA (upgradient) and WB (downgradient) - were studied, covering areas of 3.7 and 3.4 ha respectively (Figures 2a, 2b; see Table 1 for site summary). The two wetlands are classified as swamps and have similar vegetation. Dominant common tree species are red ash (*Fraxinus pennsylvanica*), sugar maple (*Acer saccharum*), white and black ash (*Fraxinus americana* and *Fraxinus nigra*), very few shrubs and herbaceous species such as jumpseed (*Persicaria virginiana*), creeping jenny (*Lysimachia struthiopteris*) and shuttlecock fern (*Matteucia struthiopteris*) (Moisan 2011). WA has an elongated shape and runs parallel to the stream which has a slope of about 0.4% in this area; it corresponds to an old meander loop (oxbow lake) visible on 1930 aerial photographs (cf. Figure 2). In contrast, WB is more rounded in shape and is connected to the river at two bends in a meander loop. The river path around this wetland has not changed significantly in the last 85 years. The river has a very low slope of approximately 0.055% in this area.

On the Matane River, the riverine wetland is located 28 km upstream from the estuary of the St. Lawrence estuary (Figure 2c; see Table 1 for site summary). The wetland is classified as a wet meadow with a shrub swamp in the portion closest to the Matane River. Dominant trees species are silver poplar (*Populus tremuloides*), swamp cedar (*Thuja occidentalis*), white spruce (*Picea glauca*) and balsam willow (*Salix pyrifolia*). Shrubs are also present with red osier dogwood (*Cornus stolonifera*) and swamp rose (*Rosa palustris*), along with herbaceous species such as spotted Joe-Pye weed (*Eupatorium maculatum* var. *maculatum*) and reed canarygrass (*Phalaris arundinacea*). The wetland covers an area of 0.062 km^2 in a zone with a channel slope of 0.25%. It occupies an elongated depression (oxbow) and a few overflow channels (Figure 2c) and is flooded regularly when groundwater levels rise in the floodplain, even when water level in the river remains below bankfull stage (Cloutier et al. 2014).

Figure 2. Field site instrumentation: a) Wetland A of the De la Roche River (flow is from right to left), b) Wetland B of the De la Roche River (flow is from top to bottom) also showing the presence of a cold spot (localized groundwater contribution) and c) Wetland on the Matane River (flow is from bottom right to top left). Note the former meander loops which are visible in the LiDAR DEM in c). The freedom space limits (defined in Biron et al. 2014) are indicated in each case with a solid black line.

Constantine et al. (2010) have shown that fine alluvium deposits can appear relatively quickly after the cutoff of a side channel, which can lead to the development of riverine wetlands. There is no evidence of such a clogging layer at the bottom of the three studied wetlands. In the Matane River, the soil is closely associated with the coarse sand/gravel that cover the floodplain. The presence of surface water is caused by groundwater flooding. In the DLR River, WB lies on low permeability clayey silt which limits water infiltration. In WA, the sediments have relatively low permeability and there was no evidence of the presence of a clogging layer.

Methods

Wetland instrumentation and monitoring

On the DLR River, three piezometer nests were hand drilled with an auger along a transect perpendicular to the river in the two wetlands (Figures 2a and 2b). Each transect position and elevation was accurately determined using a differential global positioning system (DGPS; Trimble R8GNN, vertical accuracy 10 mm) to produce a digital elevation model of each wetland. WA topography has values ranging from 33 to 38 m close to the piezometers (Figure 3a). WB is flatter with an elevation of approximately 31 m throughout the entire area (Figure 3b). The transects have a length of 110 and 190 m for WA and WB, respectively. Piezometers were made of 25.4 mm ID PVC pipes sealed at the base and equipped with 0.30 m screens at the bottom end, reaching a total depth of 3.15 m (Figure 3). A river stage gauge was installed at the riverbed, adjacent to each wetland transect (Figures 2a and 2b). Within each shallow piezometer, a Solinst pressure transducer (LTC Levelogger Junior) was installed to measure the water level and temperature every 15 min. Water level and temperature were also measured in the DLR River at 15 min intervals (LTC Levelogger Junior, accuracy of 10 mm). The time period analyzed in this paper is between June and October 2012 (data acquisition began before and continued after this period). The exact positions of the Solinst sensors were obtained with the DGPS. The water level time-series were corrected for barometric pressure recorded with a Solinst Barologger located at WB.

On the Matane River, an array of 11 piezometers was installed in the floodplain and wetland by Cloutier et al. (2014). A subset of seven of these piezometers were used in the current study (Figure 2c; piezometer names correspond to distance from the river, as in Cloutier et al. 2014). Piezometer locations were measured using a Magellan ProMark III DGPS (vertical accuracy 10 mm). A LIDAR survey (33 mm vertical accuracy) was used to obtain a high resolution map of topography. Piezometers are made from 38 mm ID PVC pipes sealed at the base and equipped with a 0.3 m screens at the bottom end. At every location, piezometers reached 3 m below the surface so that the bottom end would always be at or below the elevation of the river bed. However, because of the surface microtopography, the piezometers extended to various depths within the alluvial aquifer (Figure 3c). A river stage gauge was installed on the riverbed, near the study site to monitor water levels in the Matane River at 15 min intervals (Figure 2c). The piezometers and the river gauges were equipped with automated loggers (Hobo U20-001, accuracy of 10 mm) for water level and water temperature measurements at 15 min intervals. The time period analyzed in this paper is between June and October 2011 (data acquisition continued after this period). The time-series were corrected for barometric pressure from a Barologger located at the study site.

Figure 3. Piezometer transects showing water table elevation (masl) for a) for the De la Roche River with wetland A (DLR-WA), b) for the De la Roche River wetland B (DLR-WB), and c) for the Matane River. The water levels are average values from the study periods on the two rivers.

Between June and October 2012, total precipitation was 558 mm at the Philipsburg weather station located near the DLR River. During the same period in 2011, total precipitation was 356 mm at the Saint-Rene weather station located near the Matane River experimental site. Air temperature measured at the Philipsburg weather station between June 20th and October 25th 2012 varied from -2.6^{o}C (October 13) and 34.6^{o}C (August 4), with an average of temperature of 17.1^{o}C. During the same period in 2011, air temperature measured at the Saint-René weather station varied from -6.1^{o}C (October 7) and 29.8^{o}C (July 4), with an average of 14.9^{o}C.

Time series analyses

On the two rivers, water level and temperature fluctuations in the river and in the piezometers were analyzed through cross-correlation analyses using the software PAST (Hammer et al. 2001). This analysis provides information on the causal relationship between the input and output time series, and can thus be used to determine the influence of one series on the other based on the lag time between the two series and on the intensity of the correlation. The analyses were used to determine autocorrelations of the time series, and the level of correlation between 1) water level in rivers and in piezometers and 2) water level in rivers and water temperature in piezometer. The entire times series were considered for the computation of the analyses. Cross-correlations performed on time series for each flood event of these time series are described for the Matane River by Cloutier et al. (2014) and on a longer time period in Buffin-Bélanger et al. (2015).

Storage calculation

To provide a quantitative estimate of wetland storage during a rain event, a simple calculation was performed where recharge (w; precipitation + river) is the product of change in water level (Δh_{tot}; measured value) and effective porosity of the sediments (n_e; estimated) (Equation 1). The change in water level from precipitation (Δh_{rain}; not measured directly) can be estimated from the ratio between the volume of precipitation (Prec; measured) and the effective porosity (Equation 2). The change in water level resulting from the river (Δh_{riv}) is the difference between the total water level variation and that from precipitation alone (Equation 3). The river contribution to water levels

(Riv; not measured) is the product of Δh_{riv} and the effective porosity (Equation 4). The supplementary storage from the river per millimeter of rain is thus calculated using Equation 5.

$$w = \Delta h_{tot} \times n_e \quad (1)$$

$$\Delta h_{rain} = Prec / n_e \quad (2)$$

$$\Delta h_{riv} = \Delta h_{tot} - \Delta h_{rain} \quad (3)$$

$$Riv = \Delta h_{riv} \times n_e \quad (4)$$

$$S_{riv} = Riv / Prec \quad (5)$$

Results

Water levels

On the DLR River near WA, the water table fluctuated synchronously with the river level (Figure 4a). The river was generally gaining compared to the entire wetland. Starting with the 59 mm event of July 23 (flow rate of 2 m^3/s) and during the summer, major rainfall events created a temporary increase in the river level beyond the elevation of the piezometers A1 and A2. For the July 23 event, the precipitation had a non-negligible impact on water levels in the three piezometers at WA (e.g. 0.33 m in 14 h for A1), considering the low river stages at that time (Figure 4a). The inversion of the river-piezometer hydraulic gradient was more marked during the fall rain events, starting with the 61 mm precipitation event of September 5, where the river levels then sometimes exceed the elevation of the water level in piezometer A3. After this event, the water level in the WA piezometers rose more markedly (1.5 m in 15 h for A1), and then decreased very gradually. This difference in reaction for a rain event of similar amplitude was not explained by rainfall intensity (8.4 mm/h in July and 5.1 mm/h in September). It could be explained by the maximum flow rate reached during the flood which was much lower in July (2 m^3/s) than in September (16 m^3/s).

Figure 4. Water level variations a) for the De la Roche River with wetland A (WA), b) for the De la Roche River with wetland B (WB), and c) for the Matane River (modified from Cloutier et al. 2014). Water levels in the Matane River are higher

than piezometer levels because the gauging station is located upstream from the piezometers. The arrows indicate the rain events illustrated in Figure 5.

In WB, the river water levels were much lower than those of the three piezometers for the early part of the summer and the aquifer response to rise in river stage was very limited. The groundwater levels gradually declined throughout the summer until the September 5 event, which induced a considerable rise in WB piezometers (with a 16 m^3/s flow rate). For this event and for the 26 mm precipitation event on October 6, levels in the river temporarily exceeded the levels in the three piezometers. Water levels in piezometer B2 reacted very little to increases in river levels. During the July 23 event, the change in piezometer levels at WB was smaller and slower than at WA (0.15 m in 50 h for B1). During the September event, the water level in the WB piezometers (Figure 5a) rose even more slowly (1.1 m in 98 h for B1).

At WB, the difference in reaction for two rain events of similar amplitude can also be explained by the presence of over-bank flow (which occurs at a river stage of 31.5 m) during the September event (WA over-bank occurs at a river stage of 34.5 m which did not occur during the summer 2012). The flood hydrograph for the September event at WB (and all the flood events in the fall of 2012) had a distinct shark fin shape (Figure 5b), even though the peak level at the gauging station located at the end of the piezometer transect (see Figure 2b) is below bankfull. The analysis of aerial photographs indicated the presence of a log jam upstream from the WB transect at the same time as the shark fin shaped hydrograph.

In contrast, on the Matane River, the water levels on the D55-D127-D257 transect (cf. Figure 3c) were approximately equal to those in the river. This was maintained throughout the 2011 summer period (on Figure 4c water levels in the Matane River were higher than piezometer levels because the gauging station is located upstream from the piezometers). Groundwater levels in the regional aquifer were higher than those in the floodplain, indicating the presence of groundwater inflow towards the river. It is not uncommon for the water table to be lowest in the floodplain in regionally gaining rivers because of high evapotranspiration rates by floodplain vegetation (Jolly 1996; Burt et al.

2002). The small water level fluctuations in the river following the July 5-7 rain event (34 mm) generated limited changes (0.22 m in 22 h for D21) in the water level of all piezometers (Figure 5c). During the 58 mm event of September 4-5 (Figure 5d), the piezometer water levels increased more considerably (e.g. 1.1 m in 53 h. In all cases, the piezometer water levels decrease rapidly following the flood peak in the river. Cloutier et al. (2014) have attributed this short rapid decrease to the passage of an underground floodwave which is further analyzed by Buffin-Bélanger et al. (2015).

Figure 5. Changes in river and piezometer water levels (masl) for both wetlands in the DLR following rain events occurring on a) July 23 2012 (59 mm), and b) September 5 2012 (61 mm); changes in river and piezometer water levels in the Matane River following rain events occurring on c) July 5-7 2011 (34 mm), and d) September 4-5 2011 (58 mm).

The contrast in hydrological connections between the three studied wetlands appears clearly in the cross-correlation analysis of the river levels and piezometer levels (Figure 6). The cross-correlation coefficients $r_{xy}(k)$ are higher in the Matane River (Figure 6b, followed by WA and WB on the DLR River (Figure 6a). The time lags are considerably different between WA and WB on the DLR River (Figure 6a). The time lag between the peak in the river and in the piezometers is the shortest for WA (6 hours), with a high $r_{xy}(k)$ value of 0.90. The maximum correlation for WB is 0.61, with a time lag of 74 hours. The time lags in WA are similar to those of the Matane River which vary from 3 to 26 hours from the closest (D55) to one of the farthest (D175) piezometers. Finally, on the Matane River, the lag time increases as the distance between the river and a given piezometer increases for the Matane River (Figure 6b).

Figure 6. Cross-correlation functions ($r_{xy}(k)$) of river water levels as input and piezometer water levels as output a) for the De la Roche River, and b) for the Matane River

Water temperature

Between the end of June and the end of August (considered as the summer period), the average daily amplitude of air temperature was 13.3°C (maximum of 19.2 °C) on the

DLR River and 11.3°C on the Matane River (maximum of 19.5 °C). This amplitude was attenuated in the river at all three sites, with average values of 6.9, 3.4 and 0.8 °C (max values of 11.6, 5.2 and 2.3°C) for WA, WB and in the Matane River respectively (Figure 7). The larger attenuation in WB compared to WA was due to the presence of a localized groundwater contribution immediately upgradient from WB (identified as "cold spot" in Figure 2b). This groundwater inflow was confirmed by Distributed Temperature Sensor (DTS) measurements and ^{222}Rn analyses not shown here (Biron et al. 2013; Needelman 2014). Interestingly, at all three sites, the amplitude of water temperature was reduced considerably from mid-September, with maximum daily amplitudes of 3, 2.5 and 1.1°C for WA, WB and the Matane River, respectively. Later in the fall, the water temperature in the river near both WA and WB was nearly identical (Figure 7a). The simultaneous attenuation was probably due to a reduction in solar radiation at that time of year, and to an increase in river flow and groundwater flow. Water temperature in the DLR River piezometers was very similar throughout the study period, i.e. it did not change with distance to the river or between WA and WB. It progressively increased throughout the summer and early fall (Figure 7a). There is less temporal variability in the river temperature in the Matane River than in the DLR River, but more variability between piezometers due to the floodplain micro-topography and to screen depths (Figure 7b).

Figure 7. Water temperature a) for the De la Roche River near wetlands A and B along with the temperatures in the piezometers of wetland A (wetland B piezometers show the same pattern), and b) for the Matane River and the piezometers.

There is no peak in cross-correlation with the DLR River wetlands where correlation between levels in the river and piezometer temperature decreases linearly with time (Figure 8a). The cross-correlation analysis between river water levels and temperature in the piezometers reveal a clear peak for all piezometers in the Matane River, with time lags ranging from 75 hours for the closest piezometer (D21), to 258-446 hours for those at intermediate distances (D55, D81, D127, D175), and up to 829 and 849 hours for the longer distances (D223 and D257) (Figure 8b).

Figure 8. Cross-correlation functions of river water levels as input and piezometer water temperature as output a) for the De la Roche River, and b) for the Matane River

Wetland storage

Wetland storage is first estimated qualitatively using the autocorrelation function of the water level time series (Figure 9), in analogy to the memory effect used in karst hydrology (cf. Larocque et al. 1998). The memory effect is a qualitative assessment of the capacity of the system to keep trace of a given event through time in its hydraulic response. The longer it takes the autocorrelation function to cross the abscissa, the larger the system memory effect. The autocorrelation functions of the river at the two DLR wetlands are very similar, crossing r(k)=0 between 1200 and 1400 h (Figure 9a). The memory effect of WA is similar to that of the river, albeit with stronger r(k) for short time lags. At WB, the memory effect is shorter with r(k)=0 between 600 and 800 h. The autocorrelation functions of the Matane River (Figure 9b) are in sharp contrast to those of the DLR River. All the time series exhibit very similar r(k) throughout the time lag interval, with the piezometers closest to the river (D21 and D55) following the river autocorrelation the closest.

Figure 9. Autocorrelation functions of river and piezometer water levels a) for the De la Roche River, and b) for the Matane River.

Wetland storage was estimated for the DLR WB and for the Matane River. The DLR WB was excluded from this exercise because results from this work show that the storage capacity of WB is from surface depressions, the volume of which was not quantified in this work. Effective porosity (n_e) of the coarse sand/gravel of the Matane River wetland is estimated to be 0.25 (Cloutier et al. 2014) while that of the sandy silt of WA is estimated to be 0.1 (Freeze and Cherry 1979). The calculation was performed for all piezometers on the two wetlands for the September rain events (2012 on the De la Roche River, and 2011 on the Matane River).

The increase in wate storage due to a rain (Δh_{rain}) event is 0.61 m for the DLR WA and is 0.23 m for the Matane River. The increased heads after a flood event (Δh_{mes}) are considerably larger in WA on the DLR River and in the Matane River, as it varies from 1.38 (A3) to 1.52 m (A1) on the DLR, and from 0.66 (D257) to 1.11 m (D21) on the Matane River. The storage capacity of the DLR WA varies from 1.26 (A3) to 1.49 (A1) mm of storage per mm of rain, and smaller than that of the Matane River wetland which varies from 1.84 (D257) to 3.78 mm (D21).

Table 2. Storage capacity on the De la Roche River for Wetland A, and on the Matane River wetland. The calculation is for the September rain events (2012 on the De la Roche River, and 2011 on the Matane River)

Discussion

Response time

The lower cross-correlation coefficients for the DLR River reveal the more limited response of the aquifer to the rising river stages. However, because the piezometer reaction during flood events varies between the summer and the fall with markedly different flow rates induced by similar rain events, a shorter period cross-correlation analysis (e.g. event-based, not performed here) is considered to better reflect differences in exchanges during a season (cf. Buffin-Bélanger et al. 2015).

To explain the different time lags in the three wetlands, it is important to note that flood events are very different in the two rivers. It is hypothesized that this difference is mainly due to the difference in the size of the watershed, but this could not be verified due to the limited number of sites. The rising limb of a flood lasted between 13 and 25 hours in the DLR River, and lasted on average 74 hours in the Matane River. The shorter time lags observed for WA and for the Matane River are explained by the coarser sediments that facilitate the transfer of the pressure wave in the riparian zone. The longer time lags for WB can be related to the longer residence times evidenced by Helton et al. (2014) during over-bank flow events. In WB, log jams probably induce an increase in water levels locally, beyond the bankfull level, resulting in over-bank flow towards the wetland. Evidence of such over-bank flow to the wetland was repeatedly observed in the upstream bend of the river which is in contact with WB. Once in the wetland, water can be stored for a period of time ranging from a few days to weeks. According to Cloutier et al. (2014), this is due to the propagation of a groundwater floodwave throughout the Matane floodplain. This is not observed in the DLR River study sites, probably because of the smaller size sediments and, for WA, because of the piezometer position relative to hydrostratigraphic pathways from the abandoned meander.

The duration of standing water within a wetland is called the hydroperiod (Hayashi and Rosenberry 2002). The hydroperiod concept is closely linked to the response time of the wetland when the river levels increase. A long response time to a rain event reflects a considerable wetland storage capacity, as well as delayed and less important downstream floods. If long response times are repeated throughout the year, it can be hypothesized that they could be associated with a long hydroperiod. The latter have been associated with increased species richness within a wetland (e.g. Snodgrass et al. 2000; Chessman and Hardwick 2014).

The cross-correlation between river water levels and temperature in the piezometers is considered as an indication of the transfer of water from the river towards the alluvial aquifer (Figure 8). The positive $r_{xy}(k)$ observed for all piezometers indicates that as the river water level increases, groundwater temperature in the floodplain also increases, and vice-versa. Because river water temperature is higher than that of the floodplain groundwater during most of the season and for most of the piezometers, this can be interpreted as an actual displacement of river water through the highly permeable floodplain when river water levels increase and when hydraulic gradients are reversed due to momentarily increased river water levels. The absence of a peak in cross-correlation in the DLR River wetlands indicates that the brief flow reversals observed after a rain event do not result in the displacement of significant water volumes from the DLR River to the river bank.

On the Matane River wetland, the average water velocity estimated from the time lag to distance relationship is similar for all the piezometers and varies from 0.23 to 0.49 m/h. This is one order of magnitude lower than the floodwave propagation velocity of 6.7-11.5 m/h and one order of magnitude higher than the estimated Darcy velocity (Cloutier et al. 2014). This could be due to a smaller effective porosity or an underestimation of the floodplain hydraulic conductivity. It could also indicate that floodwave propagation and groundwater displacement are superimposed in the floodplain.

Wetland storage

Water storage is often cited as an important hydrologic function of different wetlands types (McKillop et al. 1999; Shook et al. 2013). Landscape position is considered to influence wetland storage and floodplain wetlands generally have a greater potential than headwater wetlands to store water and reduce flooding (Acreman and Holden 2013). Quantifying the volume of stored water within a floodplain or riverine wetland during a flood event is nevertheless a challenge. Considering autocorrelations of the water level time series and memory effects provide a qualitative assessment of the type of river-wetland-aquifer connections. On the DLR, the memory effect at WA is similar to that of the river, which can be interpreted as reflecting a bank storage. The shorter memory in WB compared to that of the river indicates a disconnection between the river and its wetland. In the Matane River, the similarity between the autocorrelation functions of all the wetland piezometers and that of the river itself reflects the fact that the highly permeable floodplain and its associated wetland have a strong hydraulic connection. The river and its wetland are strongly connected hydraulically, and during rain events the floodplain acts as a prolongation of the river bed.

The measured water level variation (Δh_{mes}) is higher than the one expected only from precipitation (Δh_{rain}) on the two wetlands (Table 2). This is considered to represent the additional input of water from the river to the floodplain during a flood event and reflects the hydrologic storage of the Matane River floodplain as an extension of the river during flood events. Although a floodwave was not observed in WA, the storage calculations could indicate that this process also occurs in WA, to a more limited extent. It is assumed that a single value of effective porosity is sufficient to describe each wetland. This parameter could vary considerably in the floodplain due to the presence of the wetlands. Here, it is considered that most of the head variations occur in the inorganic sediments, but this was not measured *in situ*.

The two connected wetlands (WA and Matane River) thus play distinct hydrological roles in storing flood water. Removing WA would probably not change in a significant way the DLR River flow rates which already react very rapidly to rain events. However, limiting activities within the river corridor could enhance wetland development and water storage, as well as contribute to attenuate floods and reduce sediment transport. Because of its larger storage capacity, removing the Matane River wetland could have a larger impact on downgradient flow rates, but this cannot be quantified with the available data.

Riverine wetland typology

Although they are of similar size, results from this study indicate that the three wetlands have distinct hydrological connections to the aquifer and to the river. During high flows, WA provides short-term overland storage during flood events while in WB, bank storage is very limited (due to low K sediments) and overland storage dominates. In the Matane River wetland, floodwave propagation occurs essentially through the floodplain, as the flood energy is partly dissipated within the coarse sediments. Storage of flood water per millimeter of rain is largest at this site. Figure 10 is derived from the typology suggested in Ramsar (2005) for bank storage and overland storage conditions, and complemented with the floodwave attenuation conditions from the Matane River. It summarizes the three exchange types observed in this study for southern Québec geological and climatologic conditions, in contrast to other attempts to establish a typology of floodplain connected channels (e.g. Riquier et al. 2015), where the focus is more on grain size than on hydrological connections. As underlined in Ramsar (2005), any given wetland may not fit exactly in a given type of connections and many wetlands can exhibit characteristics of more than one type. The typology presented here is expected to reflect end-members in a wide range of possible conditions.

Figure 10. Typical river-wetland-aquifer connections with a) bank storage, b) overland storage, and c) flood wave attenuation (adapted from Ramsar 2005). P is precipitation, E is evaporation, L is lateral inflow, D is drainage, OB is over-bank flow, GS is groundwater seepage, GD is groundwater discharge, and GR is groundwater recharge

This contrast between wetlands raises questions about whether or not the role of riverine wetlands can be generalized when managing rivers. Hydraulic conductivity is clearly a key variable regulating river-wetland-aquifer exchanges, as illustrated by the close connection between piezometer and river level in the Matane River highly permeable coarse sand/gravel floodplain, and the quasi-absence of connection in the DLR WB where clayey silts are present. Reach geomorphology appears linked with material permeability, with more flow exchanges in the DLR WA and in the Matane River where abandoned meanders loops have deposited permeable material (cf. Figure 2). The stable reach of the DLR WB is characterized by lower permeability materials which greatly limit hydraulic connections. In the DLR WA and Matane River reaches, meandering lateral migration and avulsion processes have contributed to deposit permeable material which, by sustaining river-aquifer exchanges, have resulted in the input of mineralized groundwater and have therefore contributed to the onset of wetland type vegetation. Locally, different states of connection between groundwater and surface water are recognized in the scientific literature and can be assessed with hydraulic conductivity and water table position (e.g.Brunner et al. 2009). At the landscape scale, the hydrologic exchanges are also controlled by the geometry and position of the stream channel within the alluvial plain (Woessner 2000). Results from this study suggest that fluvial meandering processes may play a larger role than previously acknowledged in determining the connections between rivers, wetlands and aquifers in the riverine corridor. The geometric position of the wetland relative to the river and the specific meandering dynamics in a variety of geological and climatic contexts are probably also important factors that drive riverine wetland-aquifer connections, but this could not be identified in the current study.

Conclusion

The objective of this research was to better understand what drives the surface water level regime in riverine wetlands. The study was performed on two southern Québec rivers of contrasted geomorphological contexts, the De la Roche River and the Matane River. Results from this work highlight the importance of the geomorphic setting in understanding similarities and differences between wetlands. The two wetlands on the De la Roche River exhibit marked contrast in hydrological connection despite similar size and geomorphic position relative to the river. This suggests that conducting a hydrogeomorphological assessment of a study zone is an essential step to understand the full extent of flow connectivity variations within riverine wetlands.

Reconnecting rivers to their floodplains and associated wetlands is a rising consideration in river management, but ecosystem services rendered by riverine wetlands may vary greatly. There is clearly a need to derive a typology of river-wetland-aquifer connectivity that goes beyond the site-specific case. This study is a first step in that direction, setting the baseline for a broadly applicable framework.

Acknowledgements

This project was funded by the Ouranos consortium on regional climatology and adaptation to climate change, as part of the ‘‘Fonds vert’’ for the implementation of the Québec Government Action Plan 2006–2012 on climate change and its measure 26 (Grant #510014-101). The authors thank three anonymous reviewers and the Associate Editor for constructive comments that helped improving significantly the overall quality of the paper.

References

Acreman, M.C. and J. Holden. 2013. How wetlands affect floods. *Wetlands*, 33:773-786.

Acreman, M.C. 2004. Impact assessment of wetlands: focus on hydrological and hydrogeological issues. Phase 2 report. Center for Ecology and Hydrology, Wallingford, U.K.

Amoros C. and G. Bornette. 2002. Connectivity and biocomplexity in waterbodies of riverine floodplains. *Freshwater Biology* 47:761-776.

Arnaud-Fassetta G., L. Astrade, É. Bardou, J. Corbonnois, D. Delahaye, M. Fort, E. Gautier, N. Jacob, J. Peiry, H. Piégay and M. Penven. 2009. Fluvial geomorphology and flood-risk management. *Géomorphologie : relief, processus, environnement* 2:109-128.

Biron, P.M., T. Buffin-Bélanger, M. Larocque, G. Choné, C.A. Cloutier, M.A. Ouellet, S. Demers, T. Olsen, C. Desjarlais, J. Eyquem, J. 2014. Freedom space for rivers: a sustainable management approach to enhance river resilience. *Environmental Management* doi 10.1007/s00267-014-0366-z

Biron, P.M., T. Buffin-Bélanger, M. Larocque, S. Demers, T. Olsen, M.A. Ouellet, G. Choné, C.A. Cloutier, M. Needelman. 2013. Espace de liberté: un cadre de gestion intégrée pour la conservation des cours d'eau dans un contexte de changements climatiques. Rapport présenté au Consortium Ouranos dans le cadre du PACC-26. 170 p.

Brunner, P., P.G. Cook and C.T. Simmons. 2009. Hydrogeologic controls on disconnection between surface water and groundwater. *Water Resources Research.* 45, W01422

Bullock, A. and M. Acreman. 2003. The role of wetlands in the hydrological cycle. *Hydrology and Earth System Sciences* 7(3): 358-389.

Buffin-Bélanger, T., P. Biron, M. Larocque, S. Taylor, G. Choné, M.A. Ouellet, C.A. Cloutier, C. Desjarlais, J. Eyquem. 2015. Freedom space for rivers: an economically viable river management concept in a changing climate. *Geomorphology* doi: 10.1016/j.geomorph.2015.05.013.

Buffin-Bélanger, T., C.A. Cloutier, C. Tremblay, G. Chaillou, M. Larocque. 2015. Dynamics of groundwater floodwaves and floodings in an alluvial aquifer. *Canadian Water Resources Journal.*

Burt, T.P., G. Pinay, F.E. Matheson, N.E. Haycock, A. Butturini, J.C. Clement, S. Danielscu, D.J. Dowrick, M.M. Hefting, A. Hillbricht-Ilkowska and V. Maitre. 2002. Water table fluctuations in the riparian zone: comparative results from a pan-European experiment. *Journal of Hydrology* 265: 129-148.

Chessman, B.C. and L. Hardwick. 2014. Water regimes and macroinvertebrate assemblages in floodplain wetlands of the Murrumbidgee River, Australia. *Wetlands*, 34:661-672.

Cloutier, C.A., T. Buffin-Belanger and M. Larocque. 2014. Controls of groundwater floodwave propagation in a gravelly floodplain. *Journal of Hydrology* 511: 423-431.

Constantine JA, Dunne T, Piégay H, Kondolf GM. 2010. Controls on the alluviation of oxbow lakes by bed-material load along the Sacramento River, California. *Sedimentology* 57(2): 389–407.

Cronin, C.M. 1977. Late-Wisconsin marine environments of the Champlain Valley (New York, Québec). *Quaternary Research* 7: 238-253.

Dennis, J.G. 1964. The geology of the Enosburg Area, Vermont. Vermont Geological Survey Bulletin No. 23. Montpelier, VT, Vermont Development Department.

Dubois, M., J.F. Martel, C. D'Auteuil, G.P. Prichonnet and M. Laithier. 2011. Le portrait du bassin versant de la baie Missisquoi. Document 3 du Plan directeur de l'eau. Organisme de bassin versant de la baie Missisquoi, 180 p.

Džubáková, K., H. Piégay, J. Riquier and M. Trizna. 2015. Multi-scale assessment of overflow-driven lateral connectivity in floodplain and backwater channels using LiDAR imagery. *Hydrological Processes* 29: 2315-2330.

Emmett, B.A., J.A. Hudson, P.A. Coward and B. Reynolds, 1994. The impact of a riparian wetland on streamwater quality in a recently afforested upland catchment. *Journal of Hydrology* 162: 337-353.

Environment Canada. 2013. «Canadian Climate Normals 1971-2000 Philipsburg Station». Online. <http://www.climate.weatheroffice.gc.ca/climate_normals/results_e.html?stnID=5431&lang=e&dCode=1&province=QUE&provBut=Search&month1=0&month2=12>. Consulted on May 7, 2013.

Freeze, R.A. and J.A. Cherry. 1979. Groundwater. Prentice Hall, Englewood Cliff.

Hammer, Ø, D.A.T. Harper and P.D. Ryan. 2001. Past: Paleontological statistics software package for education and data analysis. *Palaeontologia Electronica* 4(1), 9.

Hayashi, M. and D.O. Rosenberry. 2002. Effects of Ground Water Exchange on the Hydrology and Ecology of Surface Water. *Ground Water* 40(3): 309-316.

Helton, A.M., G.C. Poole, R.A. Payn, C. Izurieta and J.A. Stanford. 2014. Relative influences of the river channel, floodplain surface, and alluvial aquifer on simulated hydrologic residence time in a montane river floodplain. *Geomorphology* 205:17-26.

Hudson P.F. 2010. Floodplain Lake Formation and Dynamics in the Lower Reaches of the Large Texas Coastal Plain Rivers: Brazos, Guadalupe, and San Antonio Rivers. Austin: Texas Water Development Board, report no. 0600010583. Online. http://www.twdb.texas.gov/publications/reports/contracted_reports/doc/0600010583/twdb-hudson-final-report_without-appen.pdf

Hudson, P.F., F.T. Heitmuller and M.B. Leitch. 2012. Hydrologic connectivity of oxbow lakes along the lower Guadalupe River, Texas: The influence of geomorphic and climatic controls on the ‘‘flood pulse concept’’. *Journal of Hydrology* 414:174-183.

Jolly, I.D. 1996. The effects of river management on the hydrology and hydroecology of arid and semi-arid floodplains, In “The effects of river management on the hydrology and hydroecology of arid and semi-arid floodplains”. Anderson, M.G., S.E. Walling and P.D. Bates [Eds.] pp. 577-609. Wiley, New York.

Kline M. and B. Cahoon. 2010. Protecting river corridors in Vermont. *Journal of the American Water Resources Association* 46(2):227-236.

Larocque, M., A. Mangin, O. Banton M. Razack and O. Banton. 1998. Contribution of correlation and spectral analyses to the regional study of a large karst aquifer. *Journal of Hydrology* 205: 217-231.

Lebuis, J., 1973. Geologie du Quaternaire de la region de Matane-Amqui- Comtes de Matane et de Matapedia. Rapport DPV-216, Ministère des Richesses naturelles, Direction générale des Mines, Gouvernement du Québec, Québec, Canada. 18 p.

Lowry, C.S., J.F. Walker, R.J. Hunt and M.P. Anderson, 2007. Identifying spatial variability of groundwater discharge in a wetland stream using a distributed temperature sensor. *Water Resources Research* 43, W10408, doi:10.1029/2007WR006145.

Marchand, P., T. Buffin-Bélanger, B. Hétu, G. St-Onge. 2014. Holocene stratigraphy and implications for fjord valley-fill models of the Lower Matane River valley, Eastern Québec, Canada. *Canadian Journal of Earth Sciences* doi: 10.1139/cjes-2013-0054

McKillop, R., N. Kouwen and E.D. Soulis. 1999. Modeling the rainfall-runoff response of a headwater wetland. *Water Resources Research* 35(4): 1165-1177.

MDDELCC (Ministère du Développement durable, de l'Environnement et de la Lutte contre les changements climatiques – Québec). 2014. www.mddep.gouv.qc.ca/eau/souterraines/sih/index.htm.

Mehrtens, C.M. and R.J. Dorsey. 1987. Stratigraphy and bedrock geology of the North-western portion of the St. Albans quadrangle and the adjacent Highgate Center quad-rangle, Vermont. Vermont Geological Survey Special Bulletin No 9, 28 p.

Moisan, C. 2011. Végétation des milieux humides de la rivière de la Roche. Rapport soumis à Marie Larocque, dans le cadre du projet Espace de liberté. Institut de re-cherche en biologie végétale (IRBV): 19 p.

Needelman, M. 2014. Assessing the role of wetlands in the river corridor through groundwater and stream interactions. MSc thesis, Université du Québec à Montréal, 64 p.

Ollero A. 2010. Channel changes and floodplain management in the meandering middle Ebro River, Spain. *Geomorphology* 117(3-4):247-260.

Piégay H., S. E. Darby, E. Mosselman and N. Surian. 2005. A review of techniques available for delimiting the erodible river corridor: A sustainable approach to manag-ing bank erosion. *River Research and Applications* 21(7) : 773-89

Phillips, J.D. 2008. Geomorphic controls and transition zones in the lower Sabine River. *Hydrological Processes* 22: 2424-2437.

Phillips, J.D. 2013. Hydrological connectivity of abandoned channel water bodies on a coastal plain river. *River Research and Applications* 29: 149-160.

Racchetti, E., M. Bartoli, E. Soana, D. Longhi, R.R. Christian, M. Pinardi and P. Viaroli. 2011. Influence of hydrological connectivity of riverine wetlands on nitrogen removal via denitrification. *Biogeochemistry* 103: 335-354.

Ramsar. 2005. Guidelines for the management of groundwater to maintain wetland eco-logical character. 9th Meeting of the Conference of the Parties to the Convention on

Wetlands (Ramsar, Iran, 1971), Kampala, Uganda, 8-15 November 2005. Available at http://www.ramsar.org/cda/en/ramsar-documents-guidelines-guidelines-for-the-20845/main/ramsar/1-31-105%5E20845_4000_0__

Riquier, J., H. Piégay and M.S. Michalkova. 2015. Hydromorphological conditions in eighteen restored floodplain channels of a large river: linking patterns to processes. *Freshwater Biology* 60: 1085-1103.

Roley, S.S., J.L. Tank and M.A. Williams. 2012. Hydrologic connectivity increases denitrification in the hyporheic zone and restored floodplains of an agricultural stream. *Journal of Geophysical Research*, 117, G00N04, doi:10.1029/2012JG001950.

Shook, K., J.W. Pomeroy, C. Spence, L. Boychuk. 2013. Storage dynamics simulations in prairie wetland hydrology models: evaluation and parameterization. *Hydrological Processes* 27: 1875-1889.

Snodgrass, J.W., M.J. Komoroski, A.L.J. Bryan and J. Burger. 2000. Relationships among isolated wetland size, hydroperiod, and amphibian species richness: Implications for wetland regulation. *Conservation Biology* 14:414-419.

Stewart, D.P. 1974. Geology for Environmental Planning in the Milton-St. Albans Region, Vermont. Vermont Geological Survey Environmental Geology No 5. Montpelier, VT, Water Resources Department.

Stewart, D.P. and P. MacClintock. 1969. The surficial geology and Pleistocene history of Vermont. Vermont Geological Survey Bulletin No. 31.

Verhoeven, J.T.A, B. Arheimer, C. Yin and M.M. Hefting. 2006. Regional and global concerns over wetlands and water quality. *Trends in Ecology and Evolution* 21:96–103.

Woessner W.W. 2000. Stream and fluvial plain groundwater interactions: rescaling hydrogeologic thought. *Ground Water* 38(3): 423-429

Tables

Table 1. Site hydrogeomorphological conditions

	DLR-WA	DLR-WB	Matane
K_{min} ($m.s^{-1}$)	$5.3x10^{-7}$	0	$2.1x10^{-5}$
K_{max} ($m.s^{-1}$)	$5.4x10^{-6}$	$4.4x10^{-7}$	$8.5x10^{-4}$
Material	Sandy silt	Clayey silt	Coarse sand/gravel
Regional aquifer	Fractured bedrock	Fractured bedrock	Sand and gravel
Wetland type	Swamp	Swamp	Wet meadow and shrub swamp
Reach morphology	Abandoned meander	Stable (80 years)	River floodplain (abandoned meander)
Min-max discharge ($m^3.s^{-1}$)	0.01 – 34.3	0.01 – 34.3	7.4 – 153.2
River width at transects (m)	20	16	55
Hydraulic setting at transect	Gaining	Gaining	Gaining

Table 2. Storage capacity on the De la Roche River for Wetland A, and on the Matane River wetland. The calculation is for the September rain events (2012 on the De la Roche River, and 2011 on the Matane River)

	DRL-WA			Matane River wetland						
	A1	A2	A3	D21	D55	D81	D127	D175	D227	D257
Δh_{tot} (m)	1.52	1.39	1.38	1.11	0.95	0.84	0.79	0.73	0.70	0.66
Δh_{rain} (m)	0.61	0.61	0.61	0.23	0.23	0.23	0.23	0.23	0.23	0.23
Δh_{riv} (m)	0.91	0.78	0.77	0.88	0.72	0.61	0.56	0.50	0.47	0.43
Riv (m)	0.09	0.08	0.08	0.22	0.18	0.15	0.14	0.12	0.12	0.11
S_{riv} (mm/mm rain)	1.49	1.28	1.26	3.78	3.10	2.62	2.41	2.15	2.02	1.84

Figure Captions

Figure 1. a) Québec Province map with location of the two study sites, b) close-up map of the Matane River site (star), and c) close-up view of the two wetlands (WA and WB) of the De la Roche River. The black square in b) and c) indicates the closest gauging station and the darker-grey area represents the watershed area.

Figure 2. Field site instrumentation: a) Wetland A of the De la Roche River (flow is from right to left), b) Wetland B of the De la Roche River (flow is from top to bottom) also showing the presence of a cold spot (localized groundwater contribution), and c) Wetland on the Matane River (flow is from bottom right to top left). Note the former meander loops which are visible in the LiDAR DEM in c). The freedom space limits (defined in Biron et al. 2014) are indicated in each case with a solid black line.

Figure 3. Piezometer transects showing water table elevation (masl) a) for the De la Roche River with wetland A (DLR-WA), b) for the De la Roche River with wetland B (DLR-WB), and c) for the Matane River. The water levels are average values from the study periods on the two rivers.

Figure 4. Water level variations a) for the De la Roche River with wetland A (WA), b) for the De la Roche River with wetland B (WB), and c) for the Matane River (modified from Cloutier et al. 2014). Water levels in the Matane River are higher than piezometer levels because the gauging station is located upstream from the piezometers. The arrows indicate the rain events illustrated in Figure 5.

Figure 5. Changes in river and piezometer water levels (masl) for both wetlands in the DLR following rain events occurring on a) July 23 2012 (59 mm), and b) September 5 2012 (61 mm); changes in river and piezometer w.ater levels in the Matane River following rain events occurring on c) July 5-7 2011 (34 mm), and d) September 4-5 2011 (58 mm).

Figure 6. Cross-correlation functions ($r_{xy}(k)$) of river water levels as input and piezometer water levels as output a) for the De la Roche River, and b) for the Matane River.

Figure 7. Water temperature a) for the De la Roche River near wetlands A and B along with the temperatures in the piezometers of wetland A (wetland B piezometers show the same pattern), and b) for the Matane River and the piezometers.

Figure 8. Cross-correlation functions of river water levels as input and piezometer water temperature as output a) for the De la Roche River, and b) for the Matane River.

Figure 9. Autocorrelation functions of river and piezometer water levels a) for the De la Roche River, and b) for the Matane River.

Figure 10. Typical river-wetland-aquifer connections with a) bank storage, b) overland storage, and c) flood wave attenuation (adapted from Ramsar 2005). P is precipitation, E is evaporation, L is lateral inflow, D is drainage, OB is over-bank flow, GS is groundwater seepage, GD is groundwater discharge, and GR is groundwater recharge.

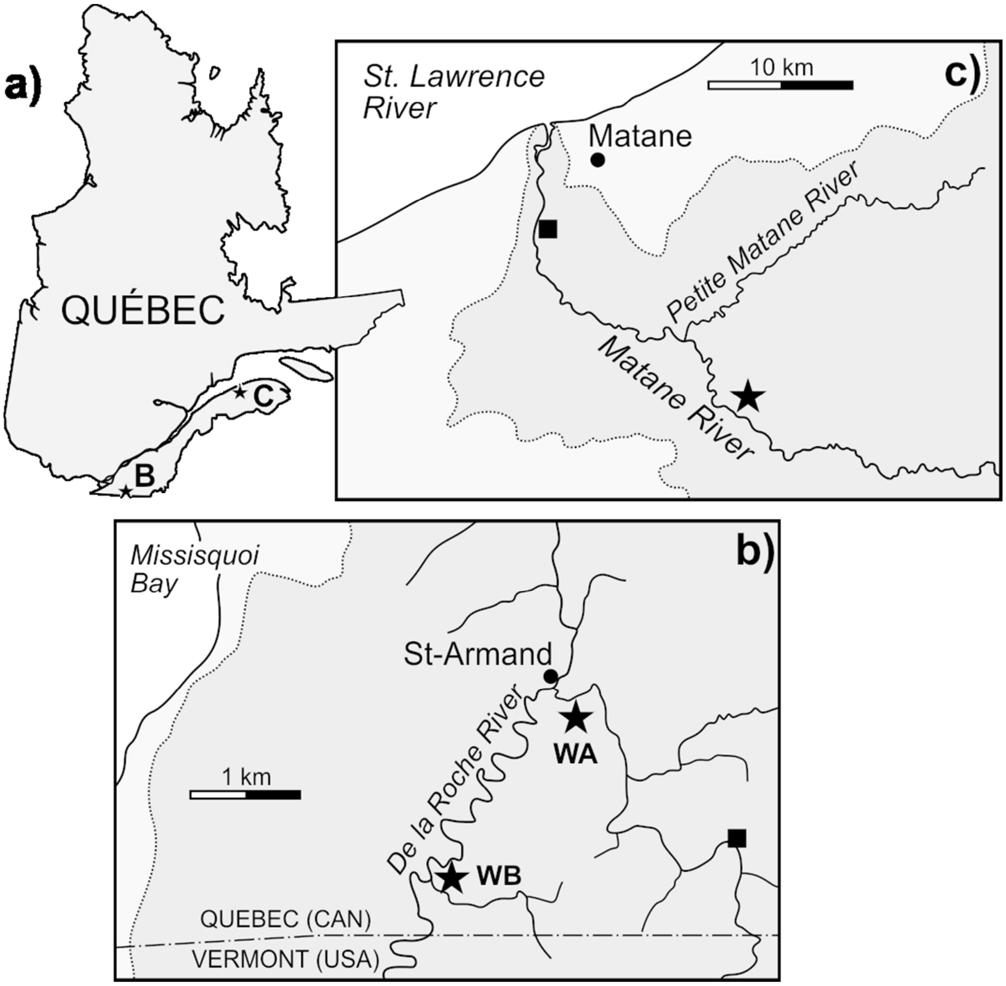

Figure 1. a) Québec Province map with location of the two study sites, b) close-up map of the Matane River site (star), and c) close-up view of the two wetlands (WA and WB) of the De la Roche River. The black square in b) and c) indicates the closest gauging station and the darker-grey area represents the watershed area.
90x88mm (300 x 300 DPI)

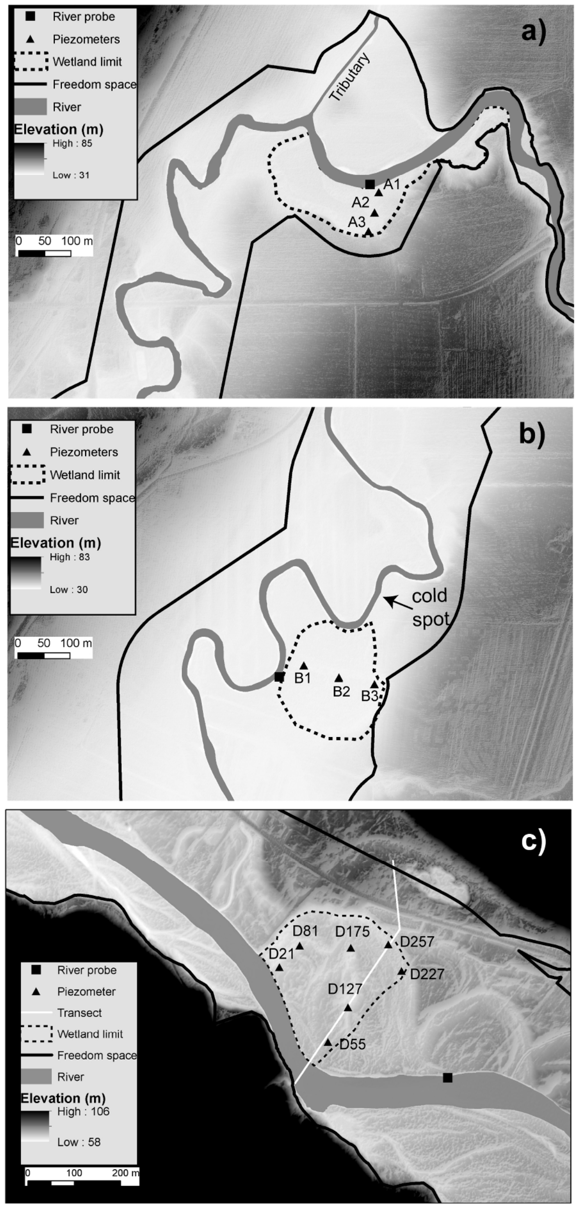

Figure 2. Field site instrumentation: a) Wetland A of the De la Roche River (flow is from right to left), b) Wetland B of the De la Roche River (flow is from top to bottom) also showing the presence of a cold spot (localized groundwater contribution), and c) Wetland on the Matane River (flow is from bottom right to top left). Note the former meander loops which are visible in the LiDAR DEM in c). The freedom space limits (defined in Biron et al. 2014) are indicated in each case with a solid black line.
124x258mm (300 x 300 DPI)

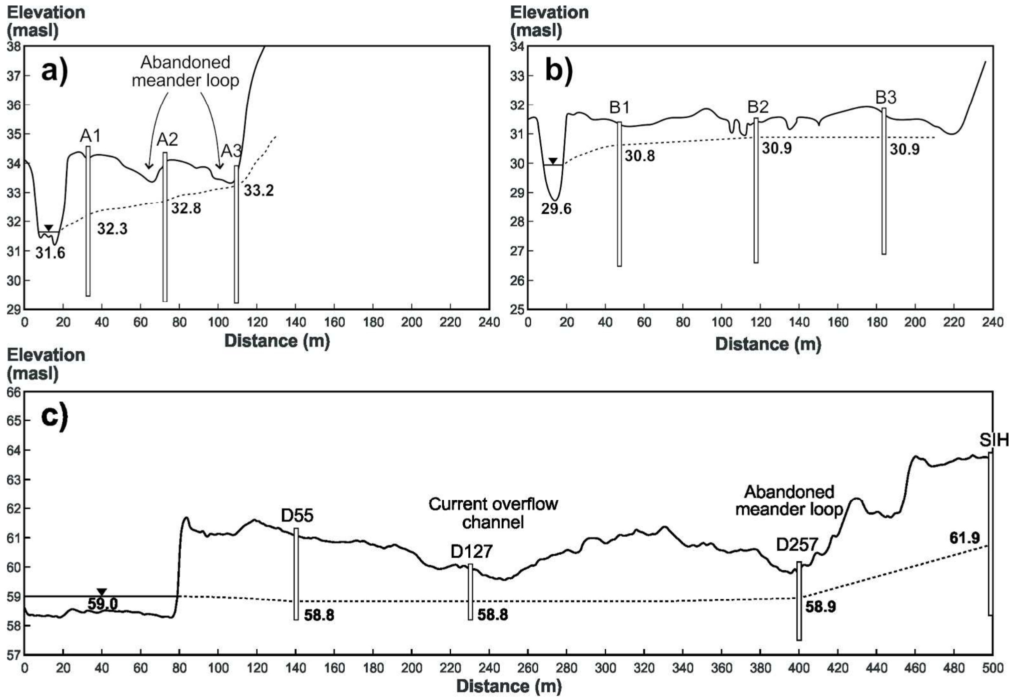

Figure 3. Piezometer transects showing water table elevation (masl) a) for the De la Roche River with wetland A (DLR-WA), b) for the De la Roche River with wetland B (DLR-WB), and c) for the Matane River. The water levels are average values from the study periods on the two rivers.
180x124mm (300 x 300 DPI)

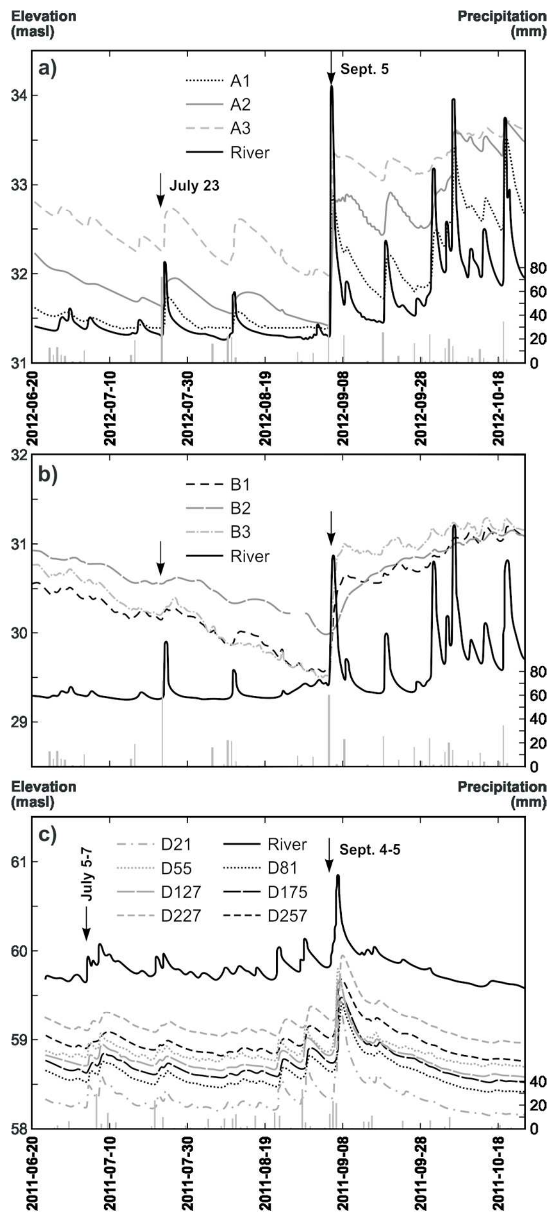

Figure 4. Water level variations a) for the De la Roche River with wetland A (WA), b) for the De la Roche River with wetland B (WB), and c) for the Matane River (modified from Cloutier et al. 2014). Water levels in the Matane River are higher than piezometer levels because the gauging station is located upstream from the piezometers. The arrows indicate the rain events illustrated in Figure 5.
90x202mm (300 x 300 DPI)

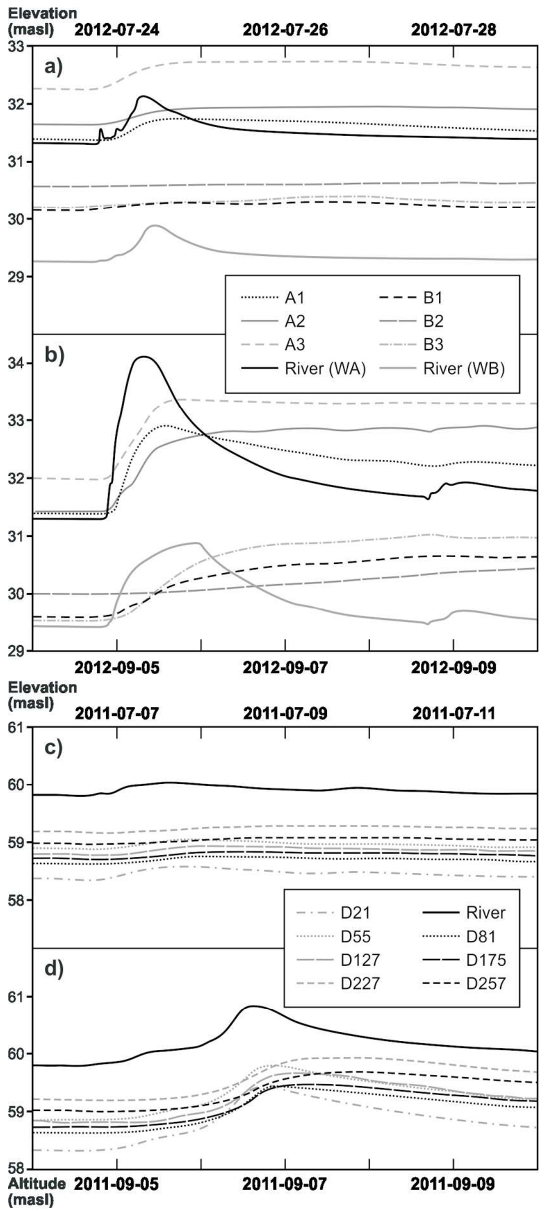

Figure 5. Changes in river and piezometer water levels (masl) for both wetlands in the DLR following rain events occurring on a) July 23 2012 (59 mm), and b) September 5 2012 (61 mm); changes in river and piezometer w.ater levels in the Matane River fol-lowing rain events occurring on c) July 5-7 2011 (34 mm), and d) September 4-5 2011 (58 mm).
90x204mm (300 x 300 DPI)

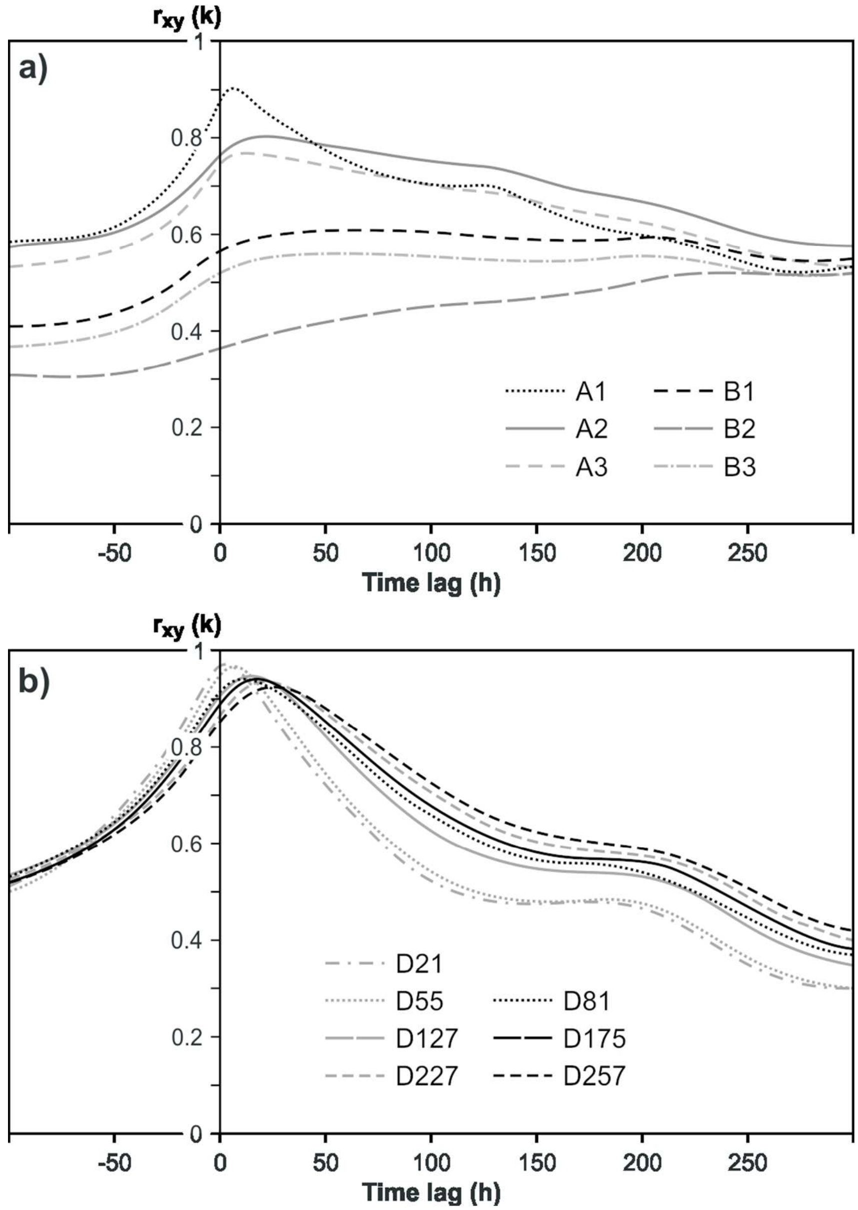

Figure 6. Cross-correlation functions (rxy(k)) of river water levels as input and piezom-eter water levels as output a) for the De la Roche River, and b) for the Matane River.
90x128mm (300 x 300 DPI)

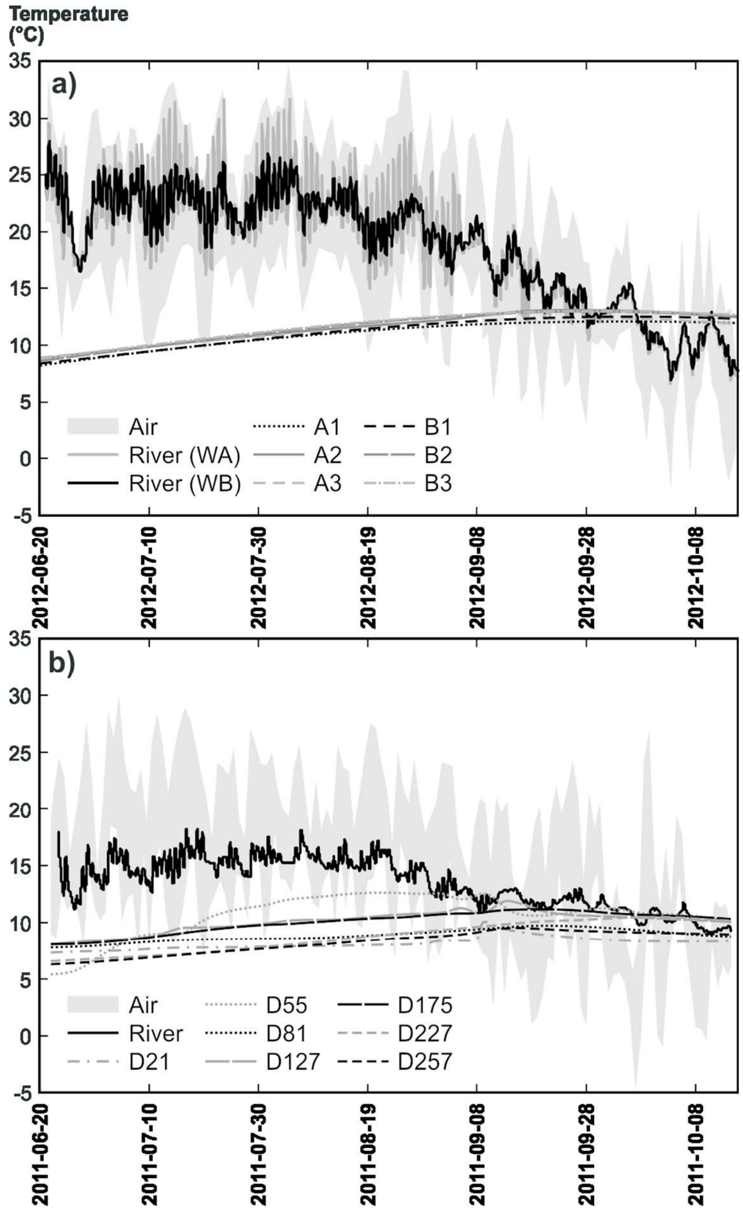

Figure 7. Water temperature a) for the De la Roche River near wetlands A and B along with the temperatures in the piezometers of wetland A (wetland B piezometers show the same pattern), and b) for the Matane River and the piezometers.
90x148mm (300 x 300 DPI)

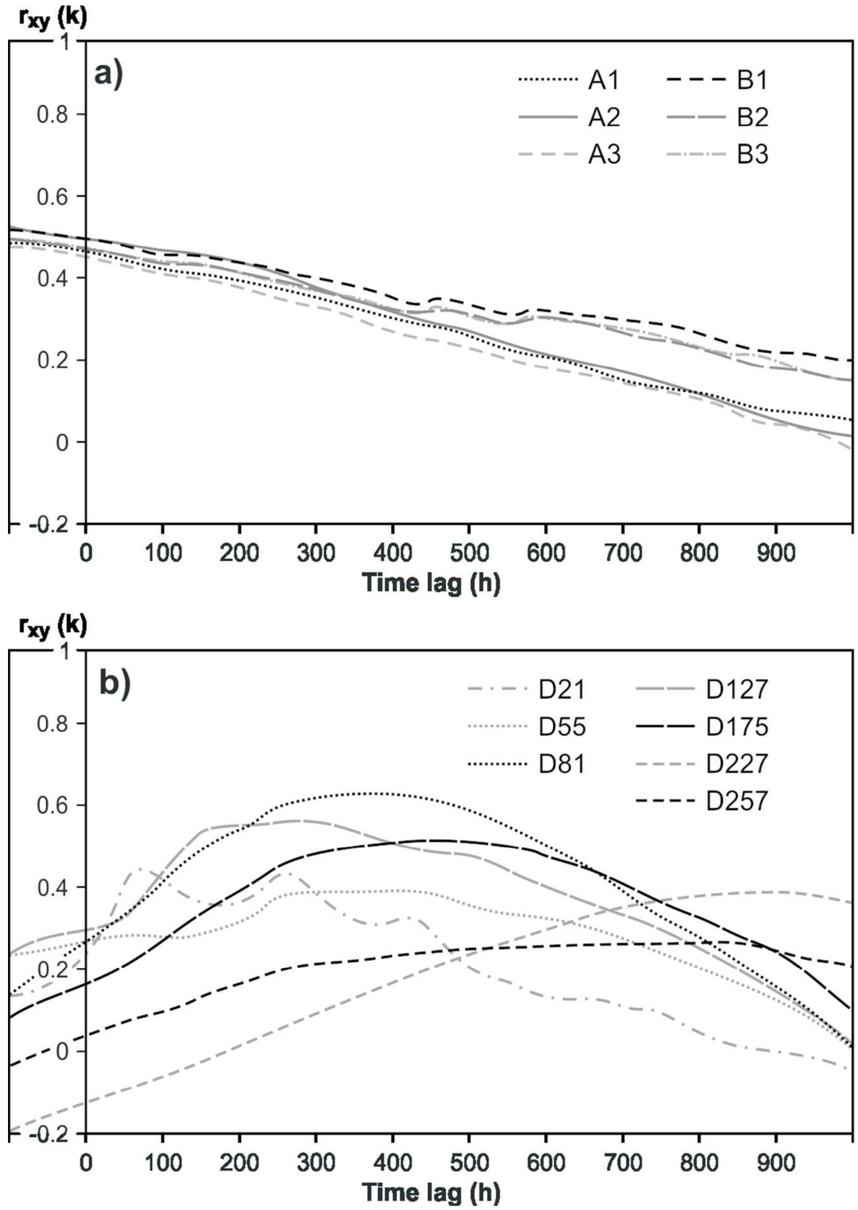

Figure 8. Cross-correlation functions of river water levels as input and piezometer wa-ter temperature as output a) for the De la Roche River, and b) for the Matane River.
90x128mm (300 x 300 DPI)

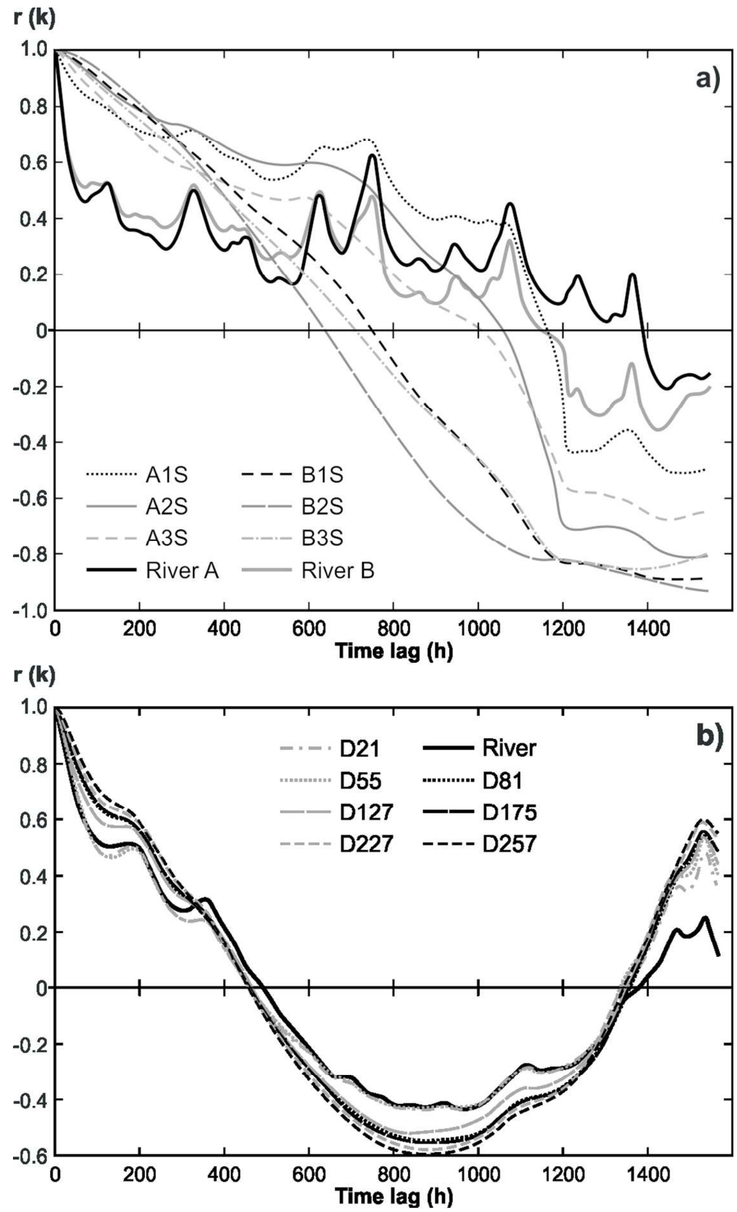

Figure 9. Autocorrelation functions of river and piezometer water levels a) for the De la Roche River, and b) for the Matane River.
90x150mm (300 x 300 DPI)

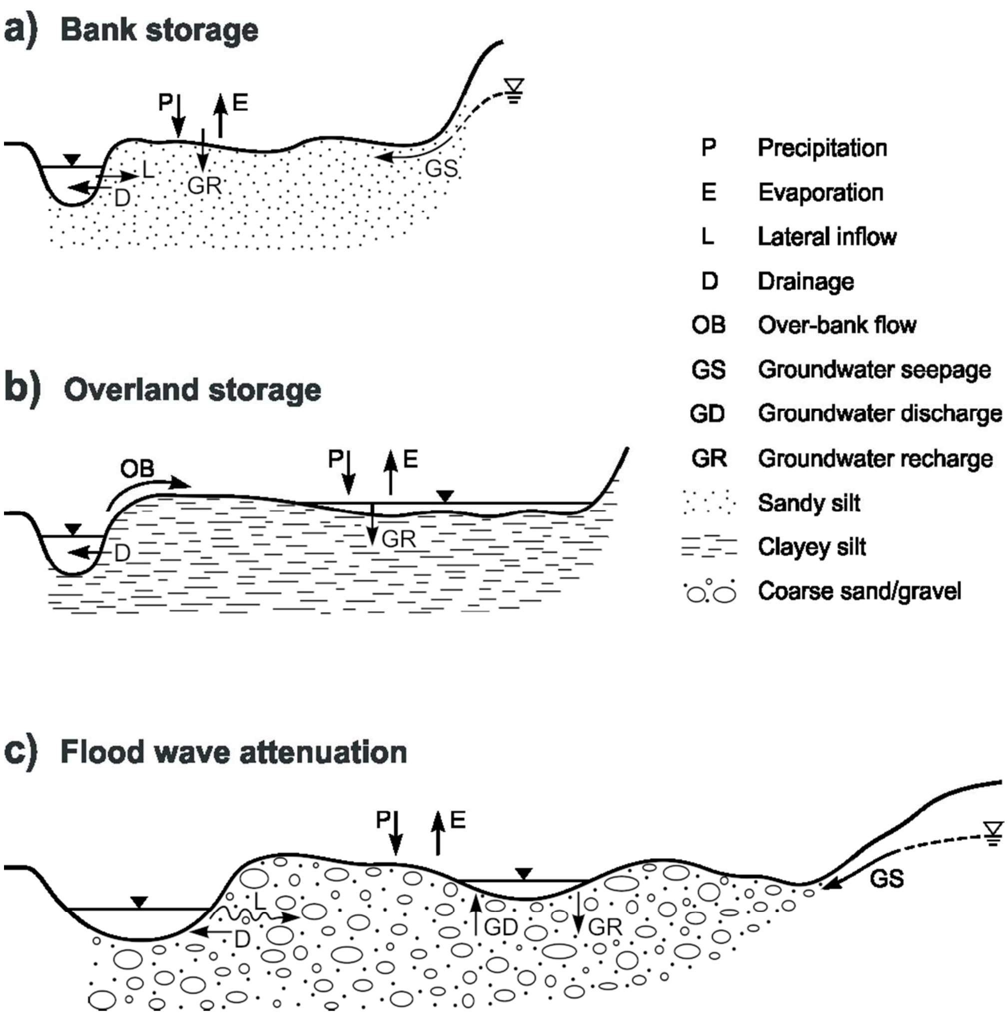

Figure 10. Typical river-wetland-aquifer connections with a) bank storage, b) overland storage, and c) flood wave attenuation (adapted from Ramsar 2005). P is precipitation, E is evaporation, L is lateral inflow, D is drainage, OB is over-bank flow, GS is groundwa-ter seepage, GD is groundwater discharge, and GR is groundwater recharge.
90x90mm (300 x 300 DPI)